Technical Notes

Brief discussions of previous investigations in the aerospace sciences and technical comments on papers published in the AIAA Journal *are presented in this special department. Entries must be restricted to a maximum of 1000 words, or the equivalent of one* Journal *page including formulas and figures. A Discussion will be published as quickly as possible after receipt of the manuscript. Neither the AIAA nor its editors are responsible for the opinions expressed by the correspondents. Authors will be invited to reply promptly.*

Analysis of Transonic Flow with Shock in Slender Hyperbolic Nozzles

C.Q. Lin* and S.F. Shen†
Cornell University, Ithaca, New York

Introduction

THE large strides made in the finite difference treatment of inviscid transonic flows in recent years have lent much confidence to its application in practical aerodynamic configurations. One of the more delicate questions, however, is the resolution of the shock, since it requires an accurate determination of a surface of discontinuity from the use of finite-sized mesh spacing. It is believed that to serve as indisputable benchmarks against which numerical schemes can be calibrated, analytical solutions of transonic flows with shock should be of fundamental interest. In Ref. 1, the well-known shockless solutions of transonic nozzle flows, e.g., Oswatitsch[2] and Hall,[3] were extended to include the presence of the shock. The shock shape was assumed to be a parabola somewhere downstream from the throat. The smooth shock turned out to require that the wall curvature be discontinuous at the shock location. For the transonic flow with shock in a smooth nozzle, the shock shape and flowfield must show singular behavior. This problem was first examined by Messiter and Adamson[4] for both two-dimensional and axially symmetric slender nozzles. The essential contribution is the introduction of an inner solution immediately behind the shock, which is matched to an outer solution valid further downstream behind the shock. This idea was later followed in Refs. 5-7 to study unsteady transonic channel flows with shock waves.

This Note amounts to a re-examination, as well as an extension beyond Ref. 4, of the steady problem, although the nozzle contour is limited to the hyperbolic. It is based on the material independently developed and presented earlier in Ref. 8. Careful comparison of Refs. 4 and 8 shows that the mathematical approaches are, indeed, essentially the same, but differ in important details. Our treatment is also somewhat broader in scope, as separate formulations are developed for the velocity potential and stream function. Consistent with our motivation, more attention is paid to the computational aspects, especially the question of numerical accuracy in the applications. Curvilinear orthogonal coordinates are used instead of the Cartesian coordinates of Ref. 4 and our expansions are carried to one term higher in all the dependent variables. The stream-function expansion, for instance, now provides a first correction for the entropy change not previously available. The set of auxiliary functions for two-dimensional case, derived in the Appendix of Ref. 8, also serve to improve the convergence of the series. Numerical results are given for a nozzle as calculated by several methods, including the present expansions for the velocity potential and the stream function, the expansion according to Ref. 4, and the results from a state-of-the-art finite difference program.

Outline of the Present Theory

Consider the two-dimensional or axisymmetric subsonic-supersonic flow near the throat of a slender hyperbolic nozzle with a shock somewhere downstream of the throat. Let (x,y) be the Cartesian coordinates with x being the axis of symmetry of the nozzle pointing downstream and y at the throat section. The half-height of the throat is taken as the unit of the length. If R denotes the radius of curvature of the wall at the throat, then $\zeta=\tan^{-1}R^{-1/2}\ll 1$ for slender nozzles. The orthogonal curvilinear coordinates (ξ,η) defined by

$$x=\sinh\delta\xi\cos\delta\eta/\sin\delta, \qquad y=\cosh\delta\xi\sin\delta\eta/\sin\delta \tag{1}$$

are further introduced, with $\eta=\pm 1$ corresponding to the upper and lower walls. Either the velocity potential or stream-function formulation is developed. For potential flow of a compressible gas, the governing equation for the velocity potential ϕ is

$$(a^2-u^2)\phi_{xx}-2uv\phi_{xy}+(a^2-v^2)\phi_{yy}(p-1)a^2\phi_y/y=0 \tag{2}$$

with boundary condition $\partial\phi/\partial\eta=0$ at $\eta=\pm 1$. In Eq. (2), u and v are the velocity components, a the speed of sound, and $p=1$ for the two-dimensional case and 2 for axisymmetric case. The outer expansion for the flows before and further downstream behind the shock is assumed to be

$$\phi(\xi,\eta)\sim K[\xi+\delta\phi_1(\xi,\eta)+\delta^2\phi_2(\xi,\eta)+\delta^3\phi_3(\xi,\eta)+\delta^4\phi_4(\xi,\eta)+\ldots] \tag{3}$$

where $K=\delta/\sin\delta$. The governing equations for $\phi_j'(j=1,2,\ldots)$ and the solution of them are given in detail in Ref. 8.

The necessity of introducing an inner expansion immediately behind the shock is due to the fact that the outer expansions on both sides of the shock cannot meet the shock condition there, because of the contradiction that the transverse pressure gradients on both sides of the shock have the same sign given by the outer solution and the normal shock condition requires that they have opposite signs. In fact, the appearance of the well-known singular behavior immediately behind the shock in the outer solution is due to the fact that the type of the governing equations is reduced to parabolic. Therefore, the scale of the streamwise coordinate for the inner expansion should be chosen such that the governing equations must remain elliptic as the flow is subsonic there. It is shown in Ref. 8 that the shock shape can be assumed to be

$$\xi_s\sim\xi_0+\delta^{3/2}g_1(\eta)+\delta^2 g_2(\eta)+\ldots \tag{4}$$

where ξ_0 denotes the one-dimensional shock position. With inner coordinate ξ^i defined by $\xi=\xi_s+\delta^{1/2}\xi^i$, the inner expansion

Received Sept. 6, 1983; revision received June 18, 1985.

*Visiting Fellow and Professor, Northwestern Polytechnical University, Xi'an, China.

†Professor, Sibley School of Mechanical and Aerospace Engineering.

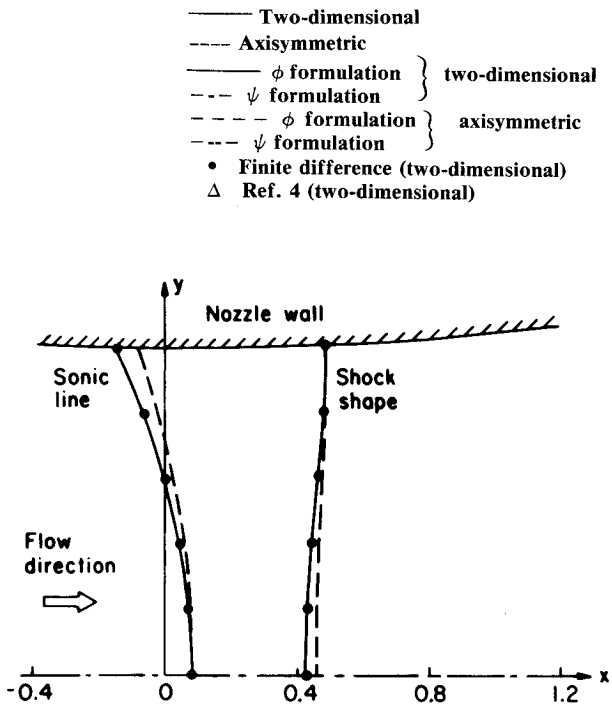

a) Shock shape and sonic line.

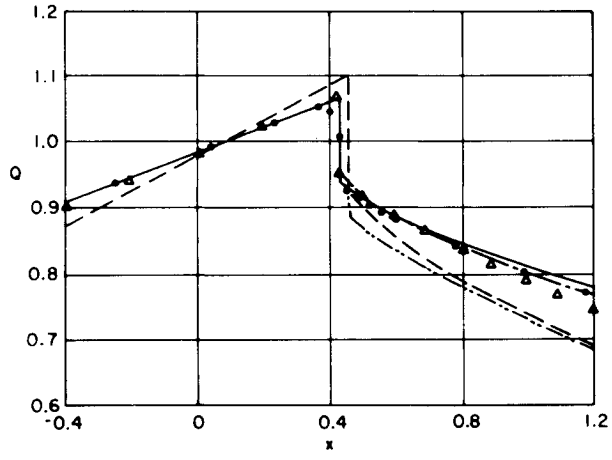

b) Velocity distribution on nozzle axis.

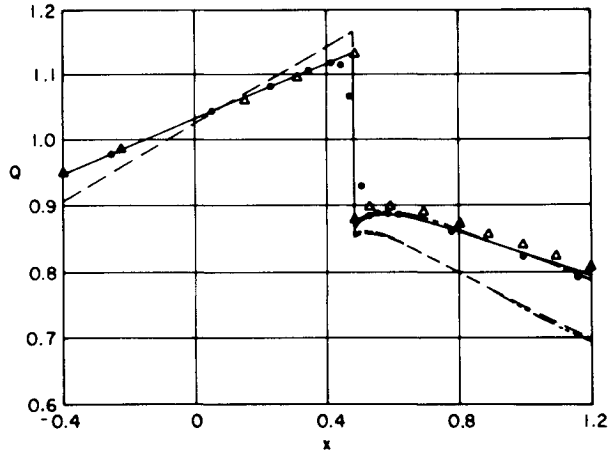

c) Velocity distribution on nozzle wall.

Fig. 1 Calculated shock shape, sonic line, and velocity distribution along nozzle axis and wall, comparison of different procedures.

for ϕ is assumed to be an ascending power series of $\delta^{1/2}$. The further details, as well as the counterpart for the streamfunction ψ formulation, are given in Ref. 8.

Numerical Examples and Comparison of Results by Different Procedures

Numerical calculation has been performed for $R=10$ and $\xi_0=0.5$ for both the two-dimensional and axisymmetric cases. Figure 1a shows the shock shape and the sonic lines, and Figs. 1b and 1c give the velocity distributions along the nozzle axis and wall. For the flow behind the shock, solutions from both the ϕ and the ψ formulations are shown for comparison. The slight discrepancy in the region reflects the different truncation errors in the asymptotic expansions. In two-dimensional case, Prof. D. Caughey has modified his finite-difference program and provided the numerical results shown in Fig. 1 for comparison. The agreement of the shock shapes in Fig. 1 is excellent.

It seems interesting to note that the shock shape in such a transonic nozzle exhibits a reversal of the curvature. In comparing the velocity distributions in the streamwise direction, the smearing of the shock due to the numerical viscosity effect in the discretization scheme is clearly seen in Fig. 1. Thus, the features in the small region of accelerating flow along the wall immediately behind the shock are much better resolved by our theory, as shown in Fig. 1. Downstream from the shock, the velocity distribution from the finite difference calculation appears to follow more closely the curve from the ψ formulation of our theory, especially for the outer region behind the shock, although Caughey's program is actually in terms of the velocity potential. In fact, in the inner solution of our theory, the accuracy for the velocity distribution is of $\mathcal{O}(\delta^{5/2})$ for both the ϕ and ψ formulations. In the outer solution of our theory, however, the accuracy for the velocity distribution is of $\mathcal{O}(\delta^3)$ for the ψ formulation, and is only of $\mathcal{O}(\xi^2)$ for the ϕ formulation. Therefore, for the velocity distribution in the outer solution behind the shock, the accuracy for the ψ formulation in our theory is better than that for the ϕ formulation and seems to be closer to the finite difference result. It should be noted, however, that by explicitly satisfying the shock conditions, a constant entropy rise of $\mathcal{O}(\delta^3)$ is considered in the present theory for the flow downstream from the shock. This effect is not present in the finite difference scheme, and thus a slight discrepancy of $\mathcal{O}(\delta^3)$ in the velocity distribution should not be unexpected.

In the two-dimensional case, the velocity distributions given by Ref. 4 are shown for comparison. The difference between the present theory and Ref. 4 is mainly due to the fewer expansion terms in Ref. 4. The comparison of the shock positions given by the two theories is shown in Fig. 2, where the scale of the x coordinate is magnified for clarity. The shock positions on the axis show some difference. One reason for the difference is

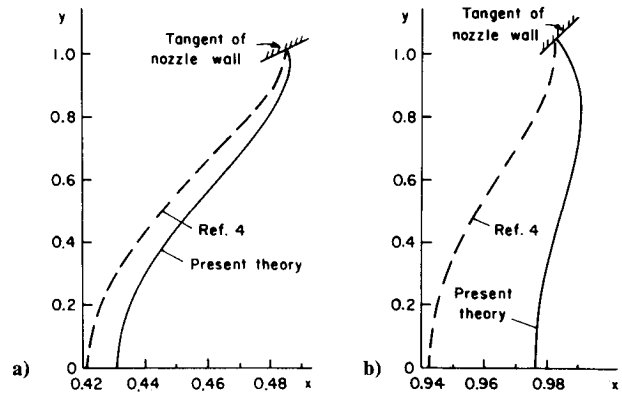

Fig. 2 Comparison of shock shapes by present theory and Ref. 4. a) $\xi_0=0.5$; b) $\xi_0=1.0$.

that, in our theory, we use one more expansion term, i.e., $\delta^2 g_2(\eta)$ in Eq. (4), which corresponds to an amount of $-(\gamma+1)\delta^2/32\xi_0$ (γ is the ratio of the specific heats) in the shock position on the axis for two-dimensional case. The second reason is that the one-dimensional shock shape $x_s = x_0$ in Ref. 4 is a straight line parallel to the y axis, whereas in our theory the one-dimensional shock shape $\xi_s = \xi_0$ is a curve determined by Eq. (1). This produces an amount of $-\sinh\delta\xi_0 \cos\delta/\sin\delta \sim \frac{1}{2}\xi_0\delta^2$ in the shock position on the axis. The latter term is also neglected in Ref. 4 which keeps terms only up to $\mathcal{O}(\delta^{3/2})$. It is noted that the tangent of the shock at the nozzle wall is perpendicular to the x axis in Ref. 4, but is properly perpendicular to the nozzle wall in our theory. It can be deduced that the total error for Ref. 4 in the shock position on the axis is $\frac{1}{2}\delta^2[\xi_0(\gamma+1)/16\xi_0]$, which is about 1% for $R=10$ and $\xi_0=0.5$ and about 4% for $R=10$ and $\xi_0=1.0$.

Acknowledgment

The authors express thanks to Prof. D. Caughey for discussion and his efforts in providing the finite difference results used in this paper and also to a reviewer of the earlier version who pointed out our oversight of Refs. 4-7.

References

[1]Lin, C.Q. and Shen, S.F., "Two-Dimensional Transonic Nozzle Flows with Shock," *AIAA Journal*, Vol. 19, Nov. 1981, pp. 1494-1496.

[2]Oswatitsch, K. and Rothstein, W., "Flow Pattern in a Converging-Diverging Nozzle," NACA TM 1215, 1949.

[3]Hall, I.M., "Transonic Flow in Two-Dimensional and Axially-Symmetric Nozzles," *Quarterly Journal of Mechanics and Applied Mathematics*, Vol. XV, Pt. 4, 1962, pp. 487-508.

[4]Messiter, A.F. and Adamson, T.C., "On the Flow Near a Weak Shock Wave Downstream of a Nozzle Throat," *Journal of Fluid Mechanics*, Vol. 69, Pt. 1, 1975, pp. 97-108.

[5]Richey, G.K. and Adamson, T.C., "Analysis of Unsteady Transonic Channel Flow with Shock Waves," *AIAA Journal*, Vol. 14, Aug. 1976, pp. 1054-1061.

[6]Chan, J.S.K. and Adamson, T.C., "Unsteady Transonic Flows with Shock Waves in an Asymmetric Channel," *AIAA Journal*, Vol. 16, April 1978, pp. 377-384.

[7]Adamson, T.C., Messiter, A.F., and Liou, M.S., "Large Amplitude Shock-Wave Motion in Two-Dimensional, Transonic Channel Flows," *AIAA Journal*, Vol. 16, Dec. 1978, pp. 1240-1247.

[8]Lin, C.Q. and Shen, S.F., "Analysis of Transonic Flow with Shock in Slender Hyperbolic Nozzles," AIAA Paper 82-0160, 1982.

Material Contravariant Components: Vorticity Transport and Vortex Theorems

Luigi Morino*
Boston University, Boston, Massachusetts

Nomenclature

g_α = base vectors, Eq. (5)
J = Jacobian of transformation $x = x(\xi^\alpha)$
t = time
v = velocity
x = vector of Cartesian components x_i
z = see Eq. (8)
ξ^α = material curvilinear coordinates
ρ = density
ω^α = material contravariant components of ω
ω = vorticity

Subscripts

i = Cartesian components
α,β = covariant components

Superscripts

α,β = contravariant components

Received Dec. 10, 1984; revision received June 5, 1985.

*Professor of Aerospace and Mechanical Engineering and Director of Center for Computational and Applied Dynamics. Member AIAA.

THE objective of this Note is to introduce the concept of material contravariant components of vorticity (that is, the contravariant components of the vorticity in a convected curvilinear coordinate system), in order to show how classical vortex theorems may be interpreted in terms of these components and to indicate how these results may be used computationally. In particular, it is shown that, for inviscid isentropic flows, the material contravariant components of the vorticity divided by the density are constant following a material point. This result simplifies the proof and the kinematic interpretation of classical results, such as vortex stretching, Kelvin's theorem, as well as the fact that vortex lines are material lines. The result is then extended to general (viscous, nonisentropic) flows, and is used to obtain a simple but powerful computational scheme for the solution of Beltrami's vorticity equation.

Mathematical Preliminaries

In order to introduce the concept of material contravariant components, consider a material (or convected) coordinate system, ξ^α, i.e., a curvilinear coordinate system that is convected with the material particles. Note that Greek letters are used for curvilinear components (subscripts for covariant and superscripts for contravariant components), and subscript i for Cartesian components. Einstein summation convention on repeated indices is used on both Greek and Latin indices.

As in the classical formulation, a given material particle is identified by the material coordinates ξ^α and at any time its location may be determined by the Cartesian coordinates x_i, functions of the material coordinates, and time

$$x_i = x_i(\xi^1, \xi^2, \xi^3, t) = x_i(\xi^\alpha, t) \qquad (i=1,2,3) \tag{1}$$

Equation (1) gives the Lagrangian description of the fluid motion. It may be noted that if ξ^α ($\alpha=1,2,3$) are kept constant, then $x_i = x_i(t)$ represents the trajectory of a fluid point. As a consequence, coordinate lines and coordinate surfaces (for instance the surface $\xi^1 = \text{const}$) are always composed of the same particles and therefore are material lines and material surfaces, respectively.

It should be emphasized that the coordinates ξ^α are closely related to the classical material coordinate X^α (see e.g., Ref. 1, p. 128) which coincide with the Cartesian coordinates x_i at $t=0$. The only difference between the X^α and ξ^α coordinates is that, in contrast with the classical approach, it is not assumed herein that the ξ^α coordinates coincide with the Cartesian coordinates at time $t=0$. This not only emphasizes the curvilinear nature of the X^α and ξ^α coordinates, but, more importantly, yields an additional flexibility that allows for a convenient choice of the ξ^α coordinates at $t=0$, thereby facilitating the derivation of the abovementioned classical results.

Next, some elementary concepts on curvilinear coordinates are briefly reviewed and applied to the specific case of material curvilinear coordinates. The velocity of a material point is